This article has been accepted for publication in a future issue of this journal, but has not been fully edited. Content may change prior to final publication. Citation information: DOI 10.1109/JLT.2014.2380439, Journal of Lightwave Technology

Wavelength-tunable dispersion compensating photonic crystal fibers suitable for conventional/coarse wavelength division multiplexing systems

Jui-Ming Hsu*, Che-Wei Yao, Jian-Zhi Chen

***Abstract*—A strongly dispersion-compensating and wavelength-tunable photonic crystal fiber (WT-DCPCF) based on a hybrid structure of dual-concentric-core photonic crystal fiber (DCC-PCF) structure and depressed-clad photonic crystal fiber (DeC-PCF) is proposed. To enhance the dispersion compensation effect, a hybrid structure of DCC-PCF and DeC-PCF is used as a basic structure. To vary the operation wavelength, some different index rods with same diameter is inserted into the central core of the hybrid fiber. The numeric results show that the operation wavelength is determined by the refractive index of the central rod, and the proposed WT-DCPCF has high chromatic dispersion coefficients of −39895 ps/km-nm to −47179 ps/km-nm at a tuned wavelength range between 1509 nm to 1610 nm. The proposed module can be used in conventional/coarse wavelength division multiplexing (CWDM) systems in optical fiber communication networks.**

***Index Terms*—Chromatic dispersion, Dispersion-compensating fiber, Dual-concentric-core fiber, Dual-concentric-core photonic crystal fiber, Photonic crystal fiber.**

I. Introduction

Chromatic dispersion in transmission fibers induces temporal optical pulse broadening, resulting in serious restrictions in transmission data rates in optical fiber communication systems. Currently, dispersion-compensating fibers (DCFs) are extensively used to minimize the negative effects of chromatic dispersion. The dispersion coefficient of conventional MCVD DCFs was approximately −100~−250 ps/km-nm [1]. J. L. Auguste et al. reported another design of MCVD DCF based on a dual-concentric core fiber (DCCF) structure with a high dispersion coefficient of −1800 ps/km-nm [2]. Additional dispersion-compensation research involved altering the air hole size or filling liquid in the holes of a specific layer of photonic crystal fiber (PCF) to design dual-concentric core PCFs (DCC-PCFs) [3–7]. We had proposed a liquid-filled hybrid structure of DCC-PCF and depressed-clad photonic crystal fiber (DeC-PCF) with an ultra-large dispersion coefficient of −40400 ps/km-nm at a wavelength of around 1550 nm [7]. The design of this hybrid structure can avoid the restriction of "mutual involvement" between two supermodes, significantly increase the index slope difference between two supermodes and thereby enlarging the dispersion coefficient.

In this work, we present a wavelength-tunable dispersion-compensating photonic crystal fiber (WT-DCPCF) based on a hybrid structure of DCC-PCF and DeC-PCF [7] in order to achieve an ultra-large dispersion coefficient as mentioned above. Furthermore, to achieve a wavelength-tunable capability, different refractive indices of Ge-doped rods (which is named as central rods in this paper) with appropriate diameter were selected to insert into the inner core of the hybrid fiber. The geometric structure of WT-DCPCFs is identical; wavelength-tuning is accomplished just by altering the Ge-doping concentration of the central rod. That greatly simplifies the process of mass production for various-wavelength DCPCFs. Ultimately, the numeric results indicated that the proposed WT-DCPCF with chromatic dispersion coefficients of −39895 ps/km-nm to −47179 ps/km-nm at a wavelength range between 1509 nm to 1610 nm, which can be tuned by the index of the central rod.

In general, a single-wavelength dispersion-compensating photonic crystal fiber (DC-PCF) [3-7] has a value of dispersion coefficient considerably larger than that of a broadband DC-PCF (B-DCPCF) [8-11]; however it is just suitable for using at a fixed wavelength. The proposed WT-DCPCF in addition to have a high dispersion coefficient close to a single-wavelength DCC-PCF, even more has an advantage of flexibility in wavelength-varying fabrication.

To fulfill the demand for high capacity of recent communications, wavelength-division multiplexing (WDM) systems are popular with telecommunications companies. WDM systems are divided into different wavelength patterns, conventional/coarse WDM (CWDM) and dense WDM (DWDM). DWDM with denser channel spacing is suitable for using a B-DCPCF to compensate the dispersion in transmission fibers. Oppositely, a cascade of the proposed WT-DCPCFs with specific different operation wavelength is quite suitable to be used for compensating dispersion in a CWDM system. Such manner can keep the length of cascaded

Manuscript received Aug. 29, 2014.

Jui-Ming Hsu, Che-Wei Yao, Jian-Zhi Chen are with the Department of Electro-Optical Engineering, National United University, Miaoli 360, Taiwan, R. O. C. (e-mails: jmhsu@nuu.edu.tw, ja519111@yahoo.com.tw, supercliff301@gmail.com).

This article has been accepted for publication in a future issue of this journal, but has not been fully edited. Content may change prior to final publication. Citation information: DOI 10.1109/JLT.2014.2380439, Journal of Lightwave Technology

WT-DCPCFs shorter than that of B-DCPCF for equivalent compensation effect due to its extremely large negative dispersion coefficient. As everyone knows that a shorter DCF not only forms a compact system, it also reduces the loss and nonlinear effect resulted in the DCF. This device has the potential for other dispersion compensating applications as well, like as a fiber laser or true time delay elements in phased array antenna systems [12], to reduce length, loss, and nonlinearity.

II. Simulation Model and Principles

The Cross-sectional view of the proposed WT-DCPCF structure is shown in Fig. 1. The cladding of the proposed WT-DCPCF consists of a triangular lattice of air holes with a diameter of d_{cl} = 0.78 μm and a pitch (center-to-center distance between the holes) of Λ = 2.50 μm in a background of undoped silica, whose refractive index can be estimated using the Sellmeier equation [13]:

$$n(\lambda) = [1 + \frac{0.6961663\,\lambda^2}{\lambda^2 - (0.0684043)^2} + \frac{0.4079426\,\lambda^2}{\lambda^2 - (0.1162414)^2} + \frac{0.8974794\,\lambda^2}{\lambda^2 - (9.896161)^2}]^{1/2}, \quad (1)$$

where λ represents the operation wavelength.

To enhance the dispersion compensating effect, a hybrid structure of DCC-PCF and DeC-PCF is used [7], that is to say, the size of holes at first layer is enlarged (d_1 = 2.00 μm). The outer ring core (ORC) with smaller-diameter air holes (d_4 = 0.68 μm), which is designed to locate at fourth layer of the WT-DCPCF, separates the cladding region into inner and outer claddings. A Ge-doped rod (central rod) with an appropriate diameter of d_{cr} = 0.90 μm, which is colored in orange in the figure, inserts into the center of inner core. The Ge-doping concentration is able to determine the refractive index (n_{cr}) of the central rod. Furthermore, the later discussion and numeric results will show that n_{cr} dominates the operation wavelength.

The chromatic dispersion coefficient D is used to quantify the amount of chromatic dispersion. $D(\lambda)$ is defined as

$$D(\lambda) = \frac{-\lambda}{c}\frac{d^2 n_{eff}}{d\lambda^2}, \quad (2)$$

where c is the speed of light in a vacuum, and n_{eff} is the effective

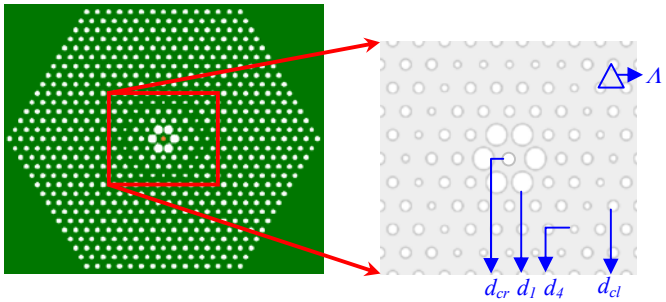

Fig. 1 Cross-sectional view of the proposed WT-DCPCF. Λ=2.50 μm, d_{cr}=0.90 μm, d_1=2.00 μm, d_4=0.68 μm, d_{cl}=0.78 μm.

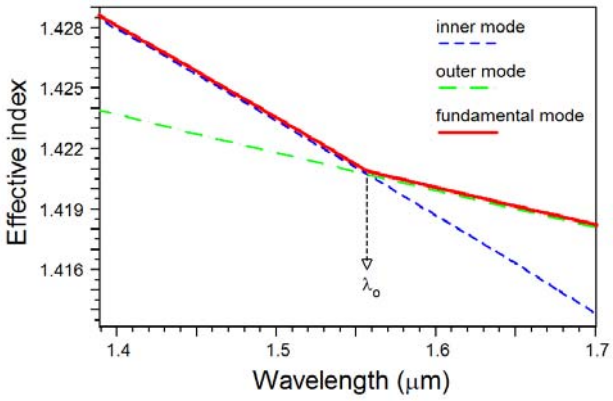

Fig. 2 Effective indices versus wavelength in a DCC-PCF.

indices of the fundamental guided modes on a fiber at various wavelengths.

According to the principle of DCC-PCF, the mode-couple effect between inner and outer modes results in a negative dispersion of the fiber at the phase-matching wavelength λ_o. The principle of DCC-PCF was described in detail in previous work [3]. For clarity, it is simplistically stated as follows. In a DCC-PCF, the effective indices of inner and outer modes, as shown in Fig. 2, are equal at λ_o. The fundamental mode coincides with the inner mode at wavelengths shorter than λ_o; thus, the propagation field is essentially confined within the central core at these wavelengths. At around the wavelength of λ_o, the field starts to spread out from the inner core to the ORC. At wavelengths longer than λ_o, the fundamental mode switches to the outer mode, meaning that most of the power is effectively guided to the ORC. According to Eq. (2), a large negative dispersion D will occur at the abruptly transitional wavelength λ_o for the fundamental mode.

III. Numerical Results and Discussions

All of the subsequent works entirely keep the geometric parameters of the WT-DCPCFs identical with the simulation model mentioned above. For clarity, the geometric parameters of all the WT-DCPCFs are listed as follows: Λ=2.50 μm, d_{cr}=0.90 μm, d_1=2.00 μm, d_4=0.68 μm, d_{cl}=0.78 μm. The only parameter varied in the subsequent simulations is the refractive index of the central rod n_{cr}.

A. Chromatic dispersion coefficients

In this work, by using the plane-wave expansion (PWE) method, the effective refractive index (n_{eff}) of the fundamental mode is first estimated. The dispersion coefficient $D(\lambda)$ is then evaluated by substituting n_{eff} into Eq. (2).

The geometric parameters are designed by consideration of minimum dispersion of the structures and modal property of the guided light. To achieve a minimum dispersion, the design of the geometric parameters Λ, d_1 and d_{cl} is based on a principle mentioned in [7]: "a large negative dispersion D will occur by increasing the index slope difference between two

This article has been accepted for publication in a future issue of this journal, but has not been fully edited. Content may change prior to final publication. Citation information: DOI 10.1109/JLT.2014.2380439, Journal of Lightwave Technology

supermodes". The d_4 is selected to coarsely adjust the minimum-dispersion wavelengths inside the telecommunication band. The d_{cl} and d_{cr} are adjusted to keep the propagation light being a single mode at the working wavelength. As regards the index of the central rod n_{cr}, we consider the dual purposes for application in Ge-doping or liquid-filling to adjust the operation wavelength, some indices of Cargille® liquids are selected as n_{cr}'s in our work.

For the proposed WT-DCPCF, Fig. 3 shows the dependence of the effective indices of inner and outer modes on wavelength for various indices of the central rod n_{cr}, the denoted refractive index n_{cr} values of the central rod are measured at their corresponding operation wavelength in this paper. The outer guide-structure is the same when the central rod is changed, therefore the effective indices of outer modes for various central rods are identical. The inflection of inner mode index-curves is a characteristic for the hybrid structure of DCC-PCF and DeC-PCF used in this work; the detail was described in [7]. The inflective curve is shown for n_{cr}=1.5146 in Fig. 3, while the inflective points of the other n_{cr}-curves are located at longer wavelengths. As shown in the figure, the larger the central rod index, the larger the effective index of inner mode, thus the longer the operation wavelength is achieved. Furthermore, the index curves of inner modes are almost parallel with each other. As mentioned previously, the value of dispersion coefficient depends upon the slope difference between the index curves of inner and outer modes. Therefore, for these examples, the dispersions should be nearly equivalent. But the dispersions are slightly different according to the numeric results that will exhibit later; this is due to two reasons: first, the index curves of inner modes are not entirely parallel with each other. Moreover, in reality the index curves of both inner and outer modes are nonlinear. It's worth noting that slope differences between the curves of inner modes and that of outer mode are considerably large as shown in the figure, this is the reason why the proposed WT-DCPCFs achieve extremely large negative dispersion coefficients.

Figure 4 indicates the dependence of the chromatic dispersion coefficients and confinement losses, which will be discussed in the later paragraph, on wavelength for various indices of the central rod. As shown in the figure, the refractive index of the central rod determines the operation wavelength. The numeric results indicate that the proposed WT-DCPCF with chromatic dispersion coefficients of −39895 ps/km-nm to −47179 ps/km-nm at a tuning wavelength range between 1509 nm to 1610 nm.

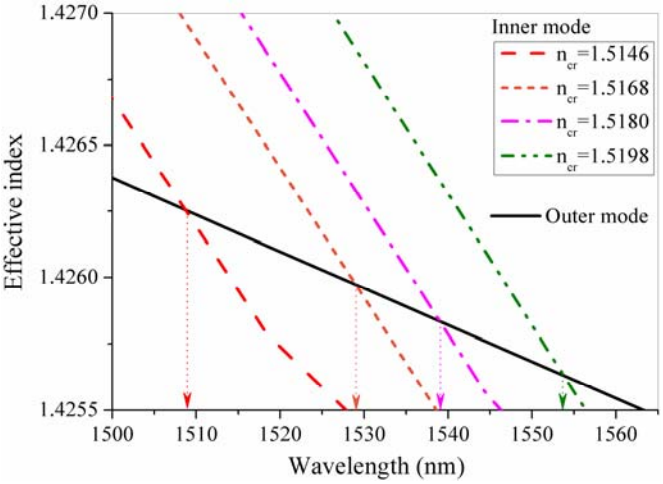

Fig. 3 Dependences of the effective indices of inner and outer modes on wavelength for various indices of the central rod in the proposed WT-DCCPCF.

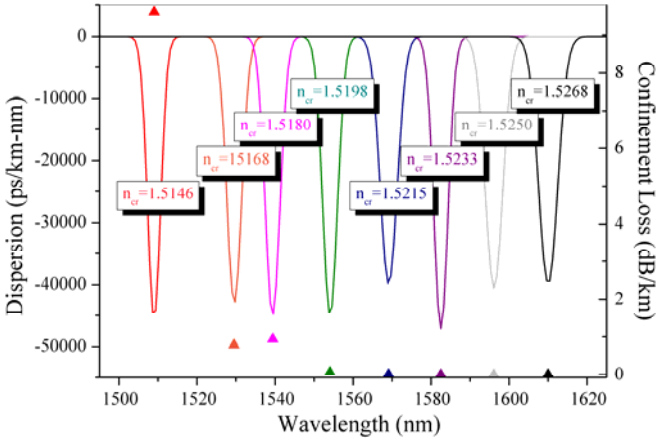

Fig. 4 Dependences of the chromatic dispersions (lines) and confinement losses (triangular symbols) on wavelength for various indices of the central rod in the proposed WT-DCPCF.

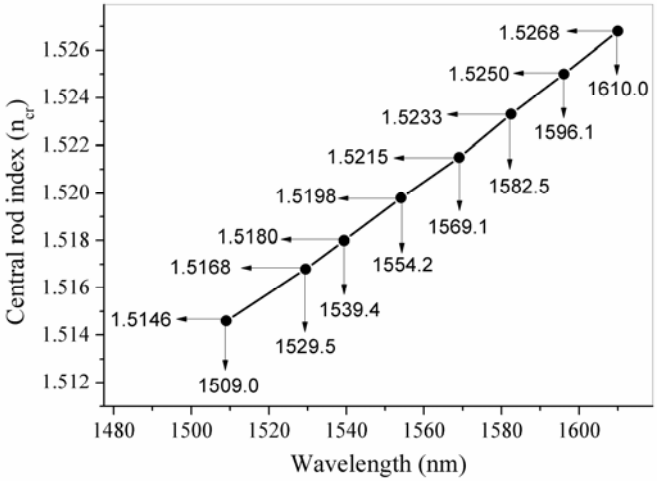

Fig. 5 Relationship between the indices of the central rod and the minimum-dispersion wavelengths for the proposed WT-DCPCF.

Figure 5 indicates the relationship between the refractive indices of the central rod and the wavelengths of the minimum dispersions shown in Fig. 4, in other words, the assigned operation wavelength in an optical communication system. The precise values of the simulated minimum-dispersion wavelengths and the rod indices are denoted in the figure. As shown in the figure, the relation curve of these two parameters is quite linear. Therefore, by using interpolation or extrapolation method at the line in Fig. 5, it is helpful for designing a WT-DCPCF with an operation wavelength excluded from the numerical results of this work.

B. *Confinement losses*

The loss is another important parameter for a DCF used in a

This article has been accepted for publication in a future issue of this journal, but has not been fully edited. Content may change prior to final publication. Citation information: DOI 10.1109/JLT.2014.2380439, Journal of Lightwave Technology

TABLE I
DETAIL NUMERIC RESULTS FOR THE PROPOSED WT-DCPCF

Central rod index	Operation wavelength (nm)	Chromatic dispersion (ps/km-nm)	Confinement loss (dB/km)
1.5268	1610.0	-39979.9	5.22×10^{-3}
1.5250	1596.1	-40606.3	3.86×10^{-3}
1.5233	1582.5	-47179.3	1.05×10^{-3}
1.5215	1569.1	-39894.9	9.04×10^{-3}
1.5198	1554.1	-45028.6	6.22×10^{-2}
1.5180	1539.4	-44988.5	9.35×10^{-1}
1.5168	1529.5	-42983.7	7.87×10^{-1}
1.5146	1509.0	-45468.6	9.61

communication link. The confinement losses at the operation wavelength for the proposed WT-DCPCF are deduced as follows. An electric field propagated in the fiber can be expressed as

$$E(x,y,z,t) = E(x,y)e^{j(kz+\omega t)+\phi} = E_o(x,y,t)e^{j(\mathrm{Re}[k]z + j\,\mathrm{Im}[k]z)} = E_o(x,y,t)e^{j\,\mathrm{Re}[k]z}e^{-\mathrm{Im}[k]z} \quad (3)$$

where $E_o(x,y,t) = E(x,y)e^{j(\omega t+\phi)}$, ϕ is an initial phase, Re[k] and Im[k] represent the real and imaginary parts of wavenumber k in the material. The k is given by

$$k = k_o \cdot n_{eff}, \quad (4)$$

where k_o is the wavenumber in free space, and n_{eff} is the effective index of the fundamental mode propagating in the fiber. In Eq. (3), $e^{j\,\mathrm{Re}[k]z}$ introduces a phase variation and $e^{-\mathrm{Im}[k]z}$ results in a loss of the electric field. Expressing the loss term in decibel:

$$Loss(dB) = 20\cdot\log(e^{-\mathrm{Im}[k]z}) = 8.686\cdot\ln(e^{-\mathrm{Im}[k]z}) = 8.686\cdot(-\mathrm{Im}[k]z). \quad (5)$$

Substituting Eq. (4) into Eq. (5), and the confinement loss denotes the loss for the electric field propagated through a unit of length. Therefore, the confinement loss (L_C) can be deduced by the value of the imaginary part of effective indices (n_{eff}) as

$$L_C = \left|\frac{Loss(dB)}{z}\right| = 8.686\cdot k_o \cdot Im[n_{eff}]. \quad (6)$$

The confinement losses of the WT-DCPCF at the simulated operation wavelengths are denoted as triangular symbols in Fig. 4. The numeric results indicate that the WT-DCPCF with confinement losses of 5.22×10^{-3} dB/km to 9.61 dB/km for the simulation cases. Fortunately, the required length of the proposed WT-DCPCF used for compensating the dispersion is quite short; therefore the confinement loss of the proposed PCFs is not serious.

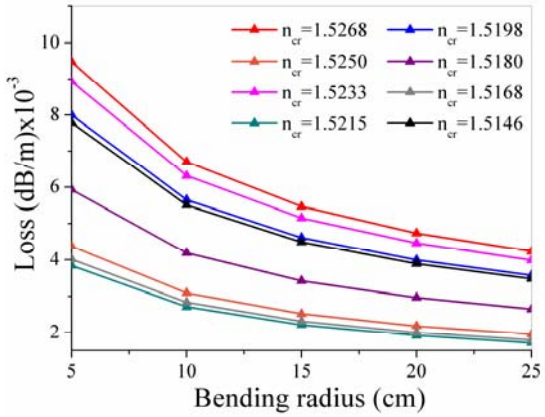

Fig. 6 Variation of bending loss with bending radius for the WT-DCPCFs with various indices of the central rod (n_{cr}).

For convenience to calculate the suitable length of WT-DCPCF to compensate the dispersion in a CWDM system, Table I lists the detail numeric results for the proposed WT-DCPCF.

C. Bending losses

When a fiber is bent, the modal field distorts outwards in the direction of the bend and a radiation loss occurs. Macro-bending losses of the proposed WT-DCPCFs can be estimated by [14]

$$\alpha(dB/m) = 4.343\sqrt{\frac{\pi}{2d_{cr}R_c}}\left[\frac{U_{eff}}{V_{eff}K_1(W_{eff})}\right]^2 \times \exp\left(-\frac{8R_cW_{eff}^3\Delta_{eff}}{3d_{cr}V_{eff}^2}\right), \quad (7)$$

where R_c is the radius of curvature of a bend in cm; U_{eff} and W_{eff} are waveguide parameters defined as $U_{eff} = k_o(d_{cr}/2)\sqrt{n_{cr}^2 - n_{eff}^2}$, $W_{eff} = k_o(d_{cr}/2)\sqrt{n_{eff}^2 - n_{FSM}^2}$; the effective normalized frequency $V_{eff} = k_o(d_{cr}/2)\sqrt{n_{cr}^2 - n_{FSM}^2}$; the relative refractive index difference $\Delta_{eff} = (n_{cr} - n_{FSM})/n_{cr}$; and $K_1(W_{eff})$ is a modified Bessel function of second kind. n_{FSM} represents the effective index of fundamental space-filling mode (FSM) in the cladding area, which can be regarded as the effective index of the cladding [15].

Bending losses of the WT-DCPCFs with various indices of the central rod are calculated for the bending radii of 5, 10, 15, 20 and 25 cm and shown in Fig. 6. It deserves to be mentioned that the bending losses for the WT-DCPCFs are estimated at their minimum-dispersion wavelengths. The numeric results indicate that the bending losses of the proposed structures are extremely small.

D. Modal considerations

To avoid the extra modal dispersion, the WT-DCPCFs have to keep the propagation light being a single mode at the working wavelength. Therefore, the modal properties of the

This article has been accepted for publication in a future issue of this journal, but has not been fully edited. Content may change prior to final publication. Citation information: DOI 10.1109/JLT.2014.2380439, Journal of Lightwave Technology

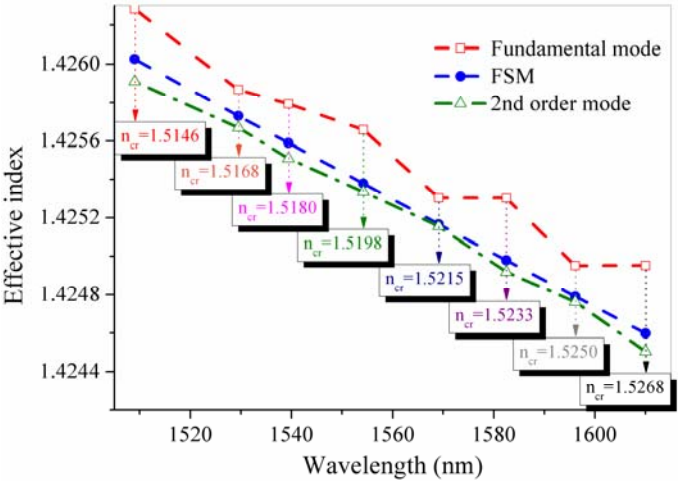

Fig. 7 Comparison between the effective indices of fundamental modes, FSMs and second order modes for the WT-DCPCFs with various indices of the central rod at their operation wavelengths.

proposed WT-DCPCFs were investigated in this work. Figure 7 compares the effective indices of the fundamental modes, the second order modes (the second order mode is the lowest mode in the high order modes, its n_{eff} should larger than that of the higher order modes) and the FSMs in the cladding area for the WT-DCPCFs at their operation wavelength. The modes should confine in the core with the condition of $n_{eff} > n_{FSM}$ while spread to the cladding for $n_{eff} < n_{FSM}$, here n_{eff} represents the effective indices of the core modes, and one can treat the n_{FSM} as the effective index of the cladding as mentioned above. As shown in Fig. 7, for all the proposed WT-DCPCFs, the effective indices of the fundamental modes satisfy the condition of $n_{eff1} > n_{FSM}$ at the operation wavelengths, it means that the fundamental modes should well-confine in the cores for the operation wavelengths. On the other hand, the effective indices of the higher order modes n_{eff2}'s meet the condition of $n_{eff2} < n_{FSM}$ for all the proposed WT-DCPCFs, that represents the high order modes will spread into the cladding. In conclusion, the proposed WT-DCPCFs all guide the light with single mode at their operation wavelengths.

IV. Fabrication Considerations

Like as the fabrication process of a general PCF, the proposed WT-DCPCF can be easily fabricated by using stack-and-draw method. The PCF preform is realized by stacking a number of capillary silica tubes and a core rod, with the same outer diameter while the different inner diameters of tubes, to form the desired air–silica structure. The core rod, just likes a traditional MCVD fiber with the core diameter of d_{cr} and the same outer diameter of other silica tubes, is formed by doping germanium into the center of silica rod. The doping concentration, which decides the refractive index of the central rod, would determine the operation wavelength of WT-DCPCF. After the stacking process, the capillaries and the core rod are held together and a WT-DCPCF as shown in Fig. 1 is then accomplished through intermediate drawing and final drawing processes.

V. Compensation Design Strategy

An ordinary single mode fiber (SMF) with zero-dispersion wavelength at 1310 nm while a dispersion of about 17 ps/km-nm at the wavelength of 1550 nm. The dispersion formula (8) describes the dispersion of the standard SMF in the wavelength range of 1200 nm to 1625 nm [16]:

$$D_{TF}(\lambda) = \frac{S_z}{4}(\lambda - \frac{\lambda_z^4}{\lambda^3}) \quad \text{ps/km-nm}, \tag{8}$$

where $D_{TF}(\lambda)$ represents the dispersion coefficient of the transmission fiber (SMF) at a wavelength of λ, zero-dispersion wavelength λ_z=1310 nm, and S_z is the value of the dispersion slope at λ_z, typical values of S_z are 0.092 ps/km-nm^2 for standard SMFs.

For WDM system, disregarding the effects of nonlinear and possible chirp in transmitter, the full compensation condition is [17]

$$D_{TF}(\lambda)L_{TF} + D_{DCF}(\lambda)L_{DCF} = 0 \tag{9}$$

where $D_{DCF}(\lambda)$ is the dispersion coefficient of the DCF versus wavelength λ, and L_{TF} and L_{DCF} are the lengths of the transmission fiber and DCF, respectively. The L_{DCF} can be expressed as

$$L_{DCF} = -L_{TF} \cdot \frac{D_{TF}(\lambda)}{D_{DCF}(\lambda)}. \tag{10}$$

Substituting Eq. (8) into Eq. (10) to yield

$$L_{DCF} = \frac{S_z L_{TF}}{4\left|D_{DCF}(\lambda)\right|}(\lambda - \frac{\lambda_z^4}{\lambda^3}). \tag{11}$$

Using Eq. (11) and the numeric results mentioned above, one can calculate the length of the WT-DCPCF in demand. As an example, a channel of CWDM system with the wavelength of 1554.1 nm, and the transmission fiber of standard SMF spans the length of 40 km. According to the numeric results listed in Table I, D_{DCF}=-45028.6 ps/km-nm at the wavelength of 1554.1 nm. Substituting the value of D_{DCF} and the other parameters S_z=0.092 ps/km-nm^2, L_{TF}=40 km, λ=1554.1 nm and λ_z=1310 nm into Eq. (11), one can estimate that the length of about 15.7 m is necessary for the WT-DCPCF with the central rod index of 1.5198. The WT-DCPCF for other channels can be designed by using the same method, and then cascaded together with each other to achieve full compensation for the CWDM system. Comparing with a B-DCPCF compensation in [10], for example, $D_{DCF}\approx -320$ and −285 ps/km-nm for the cases of Λ=0.85 and 0.90 μm respectively. Substituting the larger dispersion coefficient of the B-DCPCF (D_{DCF}=−320 ps/km-nm) into Eq. (11), the required length of the B-DCPCF is 1921 m, which is about 122 times that of the proposed WT-DCPCF. In other words, one can compensate more than 122 channels of CWDM using WT-DCPCF with total length equivalent to using a B-DCPCF.

VI. Conclusions

This study proposes a wavelength-tunable dispersion compensating photonic crystal fiber (WT-DCPCF) with an ultra-large negative dispersion coefficient. The operation wavelength is determined by the refractive index of the central rod in the core. The numeric results show that the proposed WT-DCPCF with chromatic dispersion coefficients of −39895 ps/km-nm to −47179 ps/km-nm at a tuned wavelength range between 1509 nm to 1610 nm by altering the index of central rod from 1.5146 to 1.5268. The simulated wavelength range covers the whole C band and great parts of L and S bands. Furthermore, the relationship between the index of the central rod and the operation wavelength is quite linear. Therefore, it can be predicted that the tunable range of wavelengths can be more widely extended by changing the doping concentration of the central rod with an index beyond the investigated range of 1.5146 to 1.5268. The proposed WT-DCPCF is especially suitable for use in CWDM systems in optical fiber communication networks. Moreover, this device has the potential for other dispersion compensating applications to reduce length, loss, and nonlinearity of PCF.

Acknowledgements

The authors thank Prof. Cheng-Ling Lee and Prof. Jing-Shyang Horng of the Department of Electro-Optical Engineering, National United University, Taiwan, for their useful discussions.

References

[1] A. M. Vengsarkar and W. A. Reed. (1993, June). Dispersion-compensating single-mode fibers: efficient designs for first- and second-order compensation. *Opt. Lett.* 18(11), pp. 924-926.

[2] J. L. Auguste, J. M. Blondy, J. Maury, B. Dussardier, G. Monnom, R. Jindal, K. Thyagarajan, and B. P. Pal. (2002, Jan.). Conception, realization, and characterization of a very high negative chromatic dispersion fiber. *Opt. Fiber Technol.* 8, pp. 89-105.

[3] F. Gerome, J. L. Auguste, and J. M. Blondy. (2004, Dec.). Design of dispersion-compensating fibers based on a dual-concentric-core photonic crystal fiber. *Opt. Lett.* 29(23), pp. 2725-2727.

[4] H. Subbaraman, T. Ling, Y. Q. Jiang, M. Y. Chen, P. Cao, R. T. Chen. (2007, June). Design of a broadband highly dispersive pure silica photonic crystal fiber. *Appl. Opt.* 46(16), pp. 3263-3268.

[5] X. Zhao, G. Zhou, S. Li, Z. Liu, D. Wei, Z. Hou, and L. Hou. (2008, Oct.). Photonic crystal fiber for dispersion compensation. *Appl. Opt.* 47(28), pp. 5190-5196.

[6] C. P. Yu, J. H. Liou, S. S. Huang, and H. C. Chang. (2008, Mar.). Tunable dual-core liquid-filled photonic crystal fibers for dispersion compensation. *Opt. Express.* 16(7), pp. 4443-4451.

[7] J. M. Hsu, G. S. Ye. (2012, Aug.). Dispersion ultra-strong compensating fiber based on a liquid-filled hybrid structure of dual-concentric core and depressed clad photonic crystal fiber. *J. Opt. Soc. Am. B.* 29(8), pp. 2021-2028.

[8] T. Fujisawa, K. Saitoh, K. Wada, and M. Koshiba. (2006, Jan.). Chromatic dispersion profile optimization of dual-concentric-core photonic crystal fibers for broadband dispersion compensation. *Opt. Express*. 14(2), pp. 893-900.

[9] S. K. Varshney, T, Fujisawa, K, Saitoh, and M, Koshiba. (2006, Apr.). Design and analysis of a broadband dispersion compensating photonic crystal fiber Raman amplifier operating in S-band. *Opt. Express.* 14(8), pp. 3528-3540.

[10] F. Begum, Y. Namihira, S. M. A. Razzak, S. Kaijage, N. H. Hai, T. Kinjo, K. Miyagi, N. Zou. (2009, Mar.). Novel broadband dispersion compensating photonic crystal fibers: Applications in high-speed transmission systems. *Opt. Laser Technol.* 41, pp. 679-686.

[11] F. Beltrán-Mejía, C. M. B. Cordeiro, P. Andrés, and E. Silvestre. (2012, Feb.). Broadband dispersion compensation using inner cladding modes in photonic crystal fibers. *Opt. Express.* 20(4), pp. 3467-3472.

[12] Y. Jiang, B. Howley, Z. Shi, Q. Zhou, R. T. Chen, M. Y. Chen, G. Brost, and C. Lee. (2005, Jan.). Dispersion-enhanced photonic crystal fiber array for a true time-delay structured X-band phased array antenna. *IEEE Photon. Technol. Lett.* 17(1), pp. 187–189.

[13] I. H. Malitson. (1965, Oct.). Interspecimen comparison of the refractive index of fused silica. *J. Opt. Soc. Am.* 55(10), pp. 1205-1209.

[14] S. K. Varshney, R. K. Sinha. (2004). Spectral response of bend loss in photonic crystal fibers. J. Laser Physics 14(5), pp. 756-759.

[15] T. A. Birks, J. C. Knight, P. St. J. Russell. (1997, July). Endlessly single-mode photonic crystal fiber. *Opt. Lett*. 22(13), pp. 961-963.

[16] G. Keiser, “Design Optimization of Single-Mode Fibers,” in *Optical Fiber Communications*, 3rd ed., Singapore: McGraw-Hill, 2000, ch. 3, sec. 5, pp. 127-129.

[17] R. J. Nuyts, Y. K. Park, P. Gallion. (1997, Jan.). Dispersion equalization of a 10 Gb/s repeater transmission system using dispersion compensating fibers. *J. Lightwave Technol.* 15(1), pp. 31-42.